Check for updates

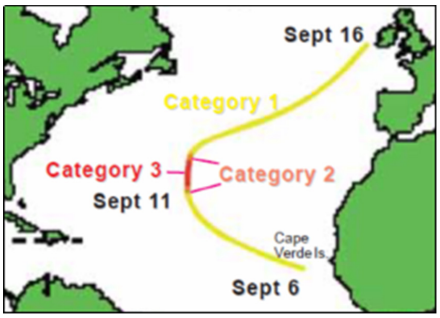

Figure 11. Hurricane Debbie track, September 1961. (Source: Met Éireann.)

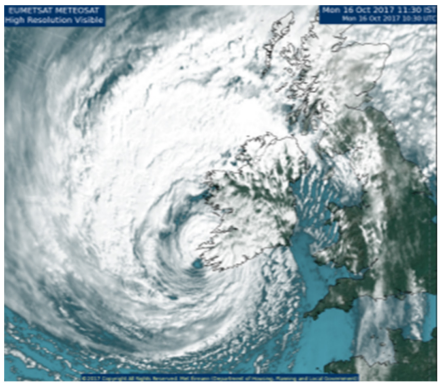

Figure 12. Is the 1130 IST (1030 UTC) EUMETSAT satellite image over Ireland showing the centre of storm Ophelia just off the Kerry Coast. The lowest mean sea level pressure at a land station during the day was 962.2hPa recorded at Valentia Observatory (County Kerry) in the hour ending 1100 IST (1000 UTC). (Source: Meteosat.)

Atlantic storms (unnamed) January 1974

The weather during January 1974 was mild, wet and stormy. There were numerous days when the winds reached storm force but two storms stand out. The storm on the evening of the 11th and morning of the 12th, and the storm on the evening of the 27th, which continued through much of the following day in Ulster. Both of these storms were associated with deep occluding depressions as they swept northwards off the west coast of Ireland and five lives were lost as a result of the two storms, along with extensive damage and coastal flooding (Aylott *et al*., 2019).

Atlantic storms (unnamed) December 1998

An intense depression continued to deepen as it moved quickly northeastwards past the northwest coast of Ireland on the evening of 26 December 1998. It was an unusually deep depression with central pressure below 950hPa. Ulster and Connaught bore the brunt of the strong winds. Maximum wind gusts reached 96kn at Malin Head, just short of the record set by 'Hurricane' *Debbie* in 1961.

Conclusions and summary

Ophelia was a significant weather event that led to widespread disruption. Long-term Irish national wind and wave records were approached, however no absolute wind or wave records were broken. Extraordinary events such as the 'Night of the Big Wind' in 1839, with hurricane strength winds, and 'Hurricane' *Debbie* in 1961 are two of Ireland's most significant storm events in recorded history. While true hurricanes are technically not found at latitudes as high as Ireland, *Debbie* retained many hurricane characteristics. Hurricane force winds are recorded on average approximately once every eight years in Ireland, but most of the time these occur in mid-winter explosively deepening mid-latitude depressions.

The utilisation of improved high resolution forecast models by Met Éireann were instrumental in declaring a 'Status Red' warning. This warning in conjunction with the State NECG advisory ensured that every effort was made to keep associated damages and losses to a minimum.

References

Aylott L, **Burt S**, **Saunders M.** 2019. Northern Ireland's longstanding record wind gust is almost certainly incorrect. *Weather* **75**: 8–13.

Burt S. 1988. The great storm of 1987. *Weather* **43**: 90–110.

Department of Housing, Local Government and Heritage. 2019. *Review report on severe weather events 2017–2018*. Dublin: Government of Ireland. https://www.gov.ie/en/publication/0c2e4-review-report-on-severe-weather-events-2017-2018/.

Graham E, **Smart D.** 2021. 'Hurricane' *Debbie* – 60 years on: a fresh analysis. *Weather* doi: 10.1002/wea.4051.

Jones S, **Harr P**, **Abraham J *et al***. 2003. The extratropical transition of tropical cyclones: forecast challenges, current understanding, and future directions. *Wea. Forecast.* **18**(6): 1052–1092.

Moore P., **Walsh L**, **Cusack E *et al***. 2018. *Storm Ophelia*. [online] Met.ie. https://www.met.ie/climate/major-weather-events [accessed 11 January 2021].

Shields L, **Fitzgerald D.** 1989. *The night of the big wind*. Dublin, Ireland: Met Éireann. https://www.met.ie/cms/assets/uploads/2017/08/Jan1839_Storm.pdf [accessed 12 January 2021].

Stewart S. 2018. *Hurricane Ophelia*. Florida, USA: National Hurricane Center. https://www.nhc.noaa.gov/data/tcr/AL172017_Ophelia.pdf [accessed 6 August 2020].

Correspondence to: P. Moore
paul.moore@met.ie
© 2021 Royal Meteorological Society
doi: 10.1002/wea.3978

Storm *Aila*: An unusually strong autumn storm in Finland

Mika Rantanen[1], Terhi K. Laurila[1], Victoria A. Sinclair[2] and Hilppa Gregow[1]

[1]*Finnish Meteorological Institute, Helsinki, Finland*
[2]*Institute for Atmospheric and Earth System Research/Physics, Faculty of Science, University of Helsinki, Helsinki, Finland*

Introduction

Extratropical cyclones (ETCs) are responsible for most of the day-to-day variability of weather in the mid-latitudes. ETCs occur most frequently in the winter season, and in favourable atmospheric conditions they can strengthen into powerful windstorms and cause significant damage to society due to their associated extreme winds. Preparing for the extreme winds caused by windstorms is crucial for many domains of society, such as forestry, insurance companies, the energy sector and power grid operators. Thus, accurately predicting the track and intensity of ETCs remains a crucial task for weather forecasters.

Although located at the tail end of the North Atlantic storm track, Finland experiences several high-impact windstorms each year (Gregow *et al*., 2020). They can occur in all seasons but typically the strongest windstorms in Finland are observed in late autumn and winter. For instance, storm *Aapeli* in January 2019 was the strongest windstorm on record in Finland with observed maximum 10min wind speed of

32.5ms^{-1} (63 kn) and a maximum wind gust of 41.6ms^{-1} (81 kn; Tollman *et al.*, 2019). Storm *Tapani* (also named as *Dagmar* in other Nordic countries) and the subsequent storm *Hannu* on the next day in December 2011 belong to the category of windstorms of greatest impact in Finland and left about 570 000 customers without electricity (Kufeoglu & Lehtonen, 2014). Windstorms can also lead to a rise of sea level and can cause damage via coastal flooding, such as during storm *Gudrun* in January 2005.

Windstorms with at least storm-force winds (>24.5ms^{-1} on the Beaufort scale) in northern Europe in the month of September are usually rare, and proportionally many of them are post-tropical cyclones (Sainsbury *et al.*, 2020). One example of these is storm *Mauri*, which developed from the remnants of Hurricane *Debby* in September 1982 and caused significant damage in northern Finland (Laurila *et al.*, 2020). In contrast, storm *Aila*, which is the topic of this paper, was a classic baroclinic storm with no tropical origins.

Storm *Aila* was an exceptionally strong autumn storm. *Aila* traversed central Finland approximately at 63°N towards the east and thus followed the track of earlier notable windstorms in Finland (see Figure 1 from Valta *et al.*, 2019). The Finnish Meteorological Institute (FMI) issued the highest level warning (red) of wind gusts and rough seas for western Finland and Bothnian Sea. The first red warnings were given with a three day lead time, which indicated strong confidence and a high predictability of the storm. At the time of the strongest winds, FMI encouraged people to stay indoors in the coastal areas. The highest observed 10-minute wind speed was 29.4ms^{-1} (57 kn) and the highest wind gust was 35.3ms^{-1} (69 kn; Figure 2). Furthermore, the strong-gale-force winds (>20.8ms^{-1} on the Beaufort scale) lasted over 15 hours in western Finland. The maximum wind gust at an inland station was 26.8ms^{-1} (52kn; FMI, 2020), and the Finnish Forest Centre (FFC) estimated the volume of forest damage to be 0.4–0.7 million m^3 (FFC, 2020). Based on preliminary estimations, *Aila* caused 160 000 households to be without electricity and altogether 2950 emergency call outs (Láng *et al.*, submitted). Additional impacts arose from unusually high precipitation totals, which in central Finland amounted to 66mmday^{-1} (FMI, 2020).

The high wind speeds observed during storm *Aila*, and the fact that the warnings could be given relatively early, is the main motivation of this study. The first objective is to give an overview of *Aila*'s synoptic development. This is performed by analysing reanalysis data. The second objective is to quantify the predictability of storm *Aila*: how early was the signal for strong winds visible in the medium-range forecasts? Finally, the third objective is to put the observed winds into a climatological larger context: how unusual was storm *Aila*? The third aim is conducted by analysing long-term weather observations from Finland and reanalysis data.

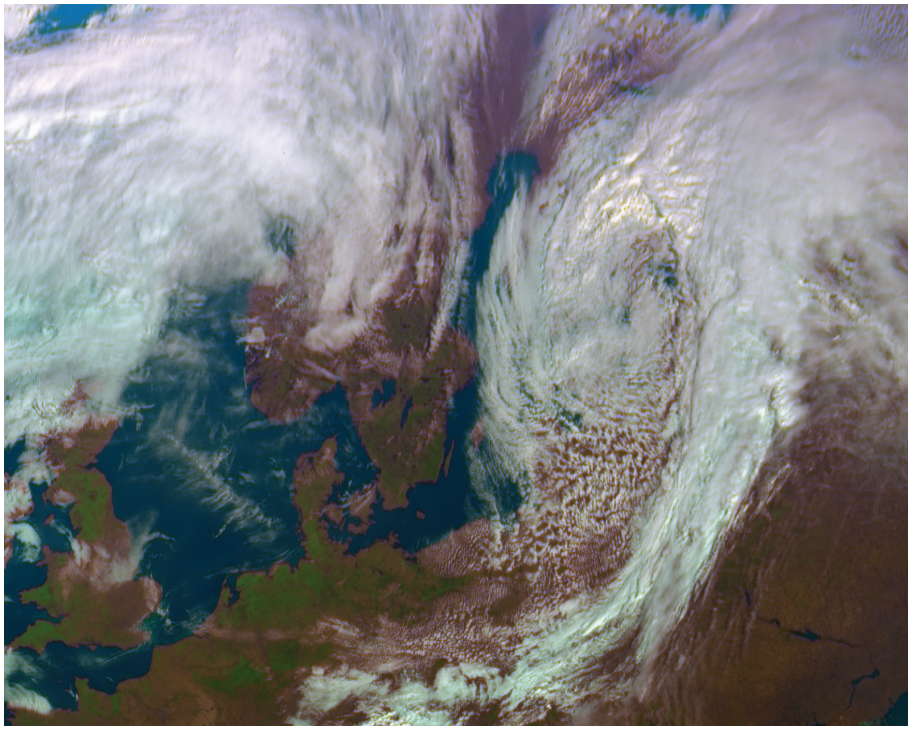

Figure 1. Satellite image of storm Aila on 17 September 2020 at 0900 UTC. Storm Aila was a high-impact autumn storm in Finland which was well predicted by medium-range forecasts. The extreme winds caused by Aila established new Finnish records for the month of September. (Source: Finnish Meteorological Institute/EUMETSAT.)

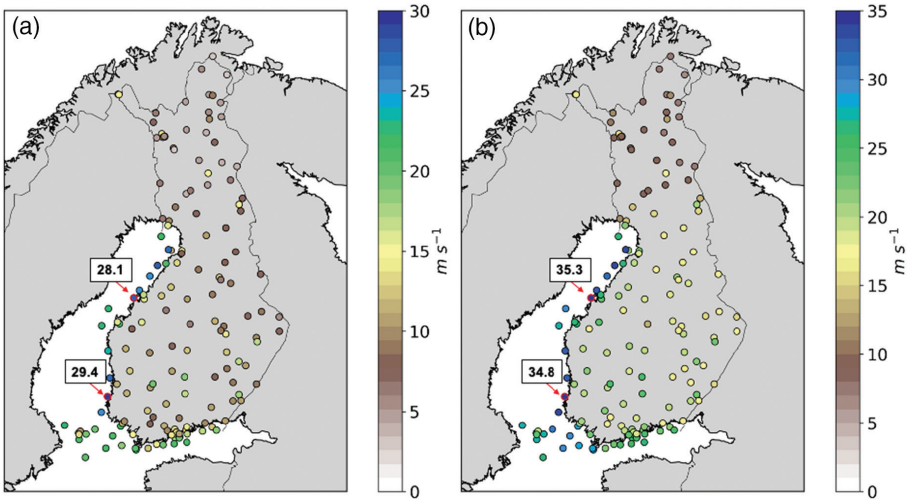

Figure 2. The observed (a) maximum wind speed and (b) maximum wind gust during 16-17 September 2020 UTC time at FMI weather stations. The two stations with the highest values (in ms^{-1}) are marked with red arrows and circles: Rauma Kylmäpihlaja (southern station) and Pietarsaari Kallan (northern station).

Data

We used ERA5 reanalysis (Hersbach *et al.*, 2020) from European Centre for Medium-Range Weather Forecasts (ECMWF) to describe the synoptic evolution of storm *Aila* and to verify the forecasts. ERA5 was used at 6-hourly temporal and 0.25° horizontal resolution. We used both surface and pressure level fields from ERA5. The fields were downloaded from Copernicus Climate Data Store (cds.climate.copernicus.eu).

The predictability of storm *Aila* was studied using high-resolution (HRES) deterministic forecasts from the Integrated Forecast System (IFS). IFS is the operational weather forecast model used by ECMWF. IFS forecasts were retrieved from ECMWF via the Meteorological Archival and Retrieval System (MARS). We used the forecasts which

were initialised at 0000 UTC and 1200 UTC on 7–18 September 2020. The original resolution of IFS HRES forecasts is 9km, which corresponds approximately to 0.1° resolution. The forecast data were regridded to 0.25° spatial resolution (31 km) which is the same resolution as the ERA5 fields that were also used.

The winds caused by storm *Aila* were analysed using wind speed and wind gust observations from FMI's weather stations located across Finland. For the climatological investigation, we analyse wind distributions from two stations where the highest winds were observed. The observational dataset includes 1-hour maximum wind speed and wind gust values during September from 2004 to 2020. Before 2004, most of the stations only recorded instantaneous values which likely missed the highest winds and hence, we use here only the 1-hour maximums which are available from 2004 onwards.

Synoptic evolution of storm *Aila*

This section gives the synoptic overview of storm *Aila*'s evolution based on ERA5 reanalysis. We describe the synoptic situation in northern Europe during 15–17 September 2020 using both low-level and upper-level meteorological variables from ERA5.

Figure 3(a) shows the initial synoptic situation in northern Europe at the time when the storm started to develop. There was a strong upper-level ridge present over central Europe (Figure 3(a)). Due to the ridge, the jet stream was shifted northward and was oriented northwest to southeast over Scandinavia. Owing to the southerly flow on western side of the ridge, the air mass in western and northwestern Europe was very warm. A weak frontal boundary north of British Isles, evident in the low-level vorticity shown in Figure 3(a), separated the warm air mass from the colder, polar air mass in Norwegian Sea (Figure 3(c)). Because of the temperature difference, the synoptic situation in the northern edge of the ridge was highly baroclinic and thus vulnerable for cyclogenesis.

The cyclogenesis started approximately on 15 September 1200 UTC when a weak upper-level trough approached the pre-existing, low-level frontal zone from the west. In Figure 3(a), the trough axis was located between Iceland and northern Scotland. Vorticity advection ahead of the upper-level trough forced ascent in the vicinity of the surface front (not shown). This mid-level ascent and associated low-level convergence caused the low-level vorticity associated with the pre-existing front to rapidly increase causing cyclogenesis to occur. This rapid spin up process can be understood both physically and mathematically by considering the 'stretching' term of the full vorticity equation (see Lackmann, 2011, section 5.3.1 for more details). Furthermore, the cyclogenesis took place in the right entrance region of the jet streak (Figure 3(a)) which enhanced the cyclone development as this region is known to be a favourable location for cyclogenesis due to enhanced upper-level divergence. As a result, a surface low pressure area formed on 15 September 1800 UTC with minimum pressure of 1013hPa (between the times in Figures 3(c) and (d); not shown).

On 16 September 2020, 0000 UTC, the low-level frontal vorticity was no longer oriented linearly, but featured as a clearly identifiable frontal wave over southern Norway (Figure 3(b)). Compared with the situation 12 hours before (Figure 3(a)), the low-level vorticity maximum had also increased. The minimum pressure of the system had decreased to 1008hPa (Figure 3(d)).

The deepening of the low pressure system continued due to the favourable phasing with the upper-level trough. On 16 September at 1200 UTC, storm *Aila* had moved to the western coast of Finland (Figure 4(a)). At this point, the strongest winds were still on the Swedish side of the Gulf of Bothnia. The intensification of the system was still in progress as indicated by the trough at 500hPa situated west from the surface low (Figure 4(a)). Thus, the structure of the system was vertically tilted which is generally a characteristic of a strengthening low pressure system. The cold-air advection west of the surface low (see northeasterly oriented isobars below the 500-hPa trough in Figure 4(a)) further contributed to the strengthening of the system by cooling the air below the trough. A decrease of thickness due to cooling causes geopotential heights to fall (decrease) at altitudes above where the maximum amount of cold advection took place, and hence deepening of the upper trough.

During the night between 16 and 17 September, storm *Aila* reached its maximum intensity in Finland. There was an upstream high pressure system to the west of *Aila* with mean sea level pressure (MSLP) greater than 1032hPa (Figure 4(b)). Thus, the pressure gradient between storm *Aila* and the high was very strong and resulted in powerful northerly airflow along the Gulf of Bothnia (Figure 4(b)). In sea areas, the wind speeds reached their maximum during the night. The flow was parallel with the Gulf of Bothnia, which presumably helped the formation of such high wind speeds because of the large fetch of open water over which the wind blew without obstruction.

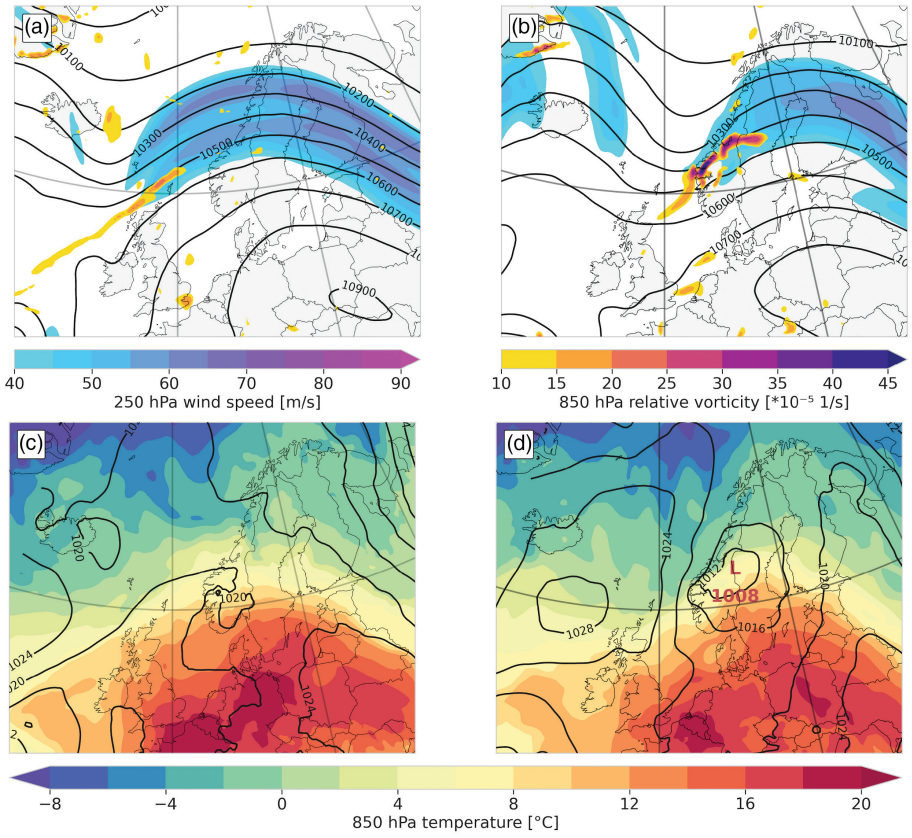

Figure 3. Synoptic situation on 15 September 2020 at 1200 UTC (left column; a, c) and 16 September 2020 at 0000 UTC (right column; b, d). In the upper row (a, b), the bluish colours show 250hPa wind speed (left-hand side colour bar), the orange colours 850-hPa relative vorticity (right-hand side colour bar) and 250hPa geopotential height is shown as black contours. In the bottom row (c, d), 850-hPa temperature is shown as colours and mean sea level pressure as black contours.

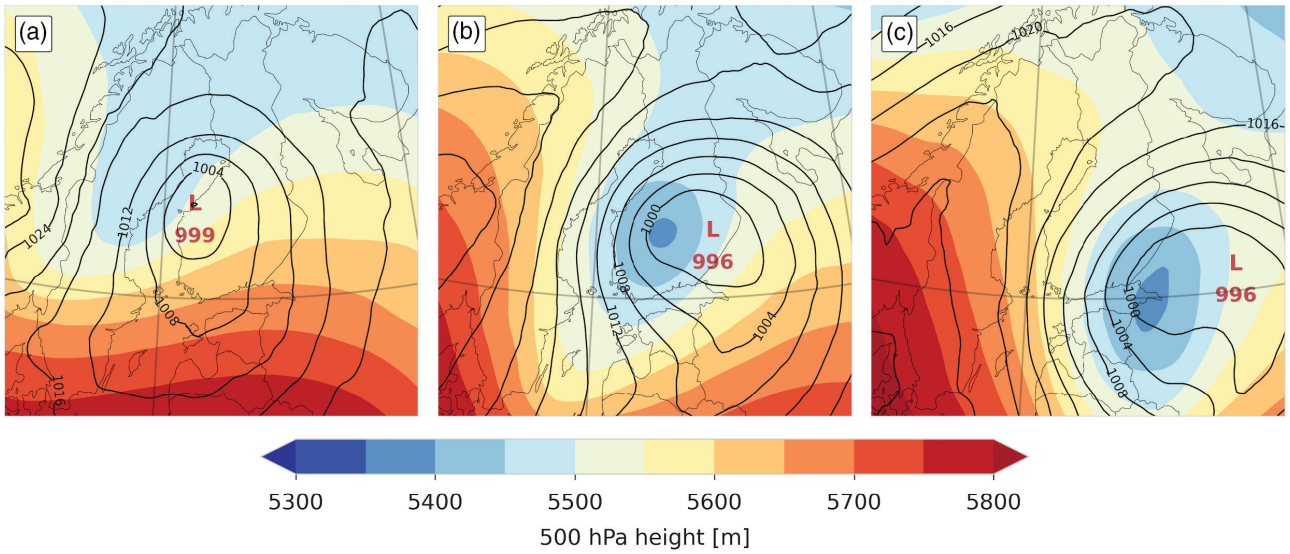

Figure 4. 500h-Pa geopotential height (colours) and mean sea level pressure (contours) on (a) 16 September 2020 at 1200 UTC, (b) 17 September 2020 at 0000 UTC and (c) 17 September 2020 at 1200 UTC.

On 17 September 1200 UTC, the storm had already reached its mature phase. The upper-level trough was detached from the main flow and formed a closed circulation (Figure 4(c)). At this point, the upper- and lower-level lows were almost vertically aligned, implying that the strengthening of the system had ceased. This is also seen by the minimum surface pressure, which did not decrease between the times shown in Figures 4(b) and (c). During the day on 17 September (Figure 4(c)), gusty winds were still blowing from the north and northeast, and caused damage especially over land areas in central Finland.

According to ERA5, the minimum surface pressure of storm *Aila* in Finland was 995hPa on 17 September 0600 UTC (between the times in Figures 4(b) and (c), not shown). The maximum 24-hour deepening rate was 16hPa and took place from 15 September 1800 UTC to 16 September 1800 UTC.

Comparison of IFS forecasts to ERA5

The first warnings of strong gale-force winds (21ms^{-1}) for western sea areas for 17 September were issued by FMI in the morning of 13 September, 4 days in advance. The highest red level warnings were issued with a lead time of three days. Thus, it was evident that storm *Aila* was quite well captured by numerical weather prediction models, as the warnings could be given so early. The medium-range forecasts by FMI are mostly based on the IFS model, which is why we next compare the IFS forecasts at different initialisation times to the ERA5 reanalysis.

In Figure 5, MSLP forecasts initialised every 12 hours between 11 September 0000 UTC and 16 September 0000 UTC by IFS are shown. The valid time of all forecasts is 17 September 0000 UTC (see ERA5 analysis in Figure 5(l)), which was approximately the time when the winds were the strongest over Finnish sea areas. Thus, the forecasts have lead times ranging from 144 hours (Figure 5(a)) to 24 hours (Figure 5(i)).

The first impression from the MSLP fields in Figure 5 is that the low pressure system is clearly visible in all forecasts. The centre of the storm varied by several hundred kilometres in consecutive forecasts at T+108 to T+144 hour lead times (Figures 5(a–e)), but after 96 hours lead time increased consistency in the location of the centre emerged (Figures 5(f–k)). However, regardless of the variability in the location of the centre, in all the forecasts a relatively strong pressure gradient in western Finland was present.

Most of the forecasts predicted too low MSLP values over southwestern Finland and too high MSLP values over eastern and northeastern Finland. This is seen as a dipole type of structure in the difference fields which appear to be present in the majority of the forecasts (Figure 5). Consequently, in these forecasts, the low pressure centre was predicted to be too far west than where it was in reality (Figure 5(l)).

The magnitude of the MSLP errors are more than 15 hPa in the T+96 to T+144 hours forecasts (Figures 5(a–e)), but after 84 hours lead time the error generally decreased and was less than 10 hPa (Figures 5(f)–(k)). The central pressure of the system was consistently predicted to be lower than the actual value (996hPa, Figure 5(l)). Only two forecasts predicted a weaker storm (Figure 5(a, d)).

Figure 6 shows the predictability of 10-metre maximum wind gust speeds for two specific areas. The x-axis of the panels describes the valid time of the forecasts, and the y-axis the lead time of the forecasts. In the case of an accurate forecast, the wind gust values (red shading) would agree with ERA5 (shown at the bottom rows in Figure 6). Figure 6 also allows us to determine the consistency of the forecasts. A high degree of consistency means the same values are predicted in multiple, consecutive forecasts which appear in Figure 6 as vertical lines of the same colour. The first area (Figure 6(a)) is located in the western coast of Finland, including quite a big fraction of the Bothnian Sea. This was the area where the strongest 10-metre average wind speed was observed (Figure 2). The second area (Figure 6(b)) is located in southern Finland, and was considered here because this was the area over land where the strongest winds were forecast.

Some early indications of the storm-force wind gusts were visible already in the T+216 to T+240 forecasts for both areas. However, the signal was not yet consistent, and partly disappeared at 192–204 hour lead time. After that, starting from 180 hours lead time, the forecast signal for stormy winds began to strengthen and became more consistent. Nevertheless, the forecasts with lead times longer than 144 hours had small timing errors (Figure 6). At 0 to 144 hours lead time, the forecasts form almost invariant vertical lines, which means that the valid times of the strongest gusts remain fixed and thus the forecasts were good. After 144 hours, the forecasts tend to drift rightward towards later valid times, meaning that the strongest winds were forecast to occur 12–24 hours later than when they did in reality.

For western Finland (Figure 6a), compared with ERA5, IFS slightly overestimated the maximum wind gusts for 17 September 0000 UTC at short (12–72 hour) lead times, which is a critical time frame for preparations and communication. In southern Finland (Figure 6(b)) on 17 September

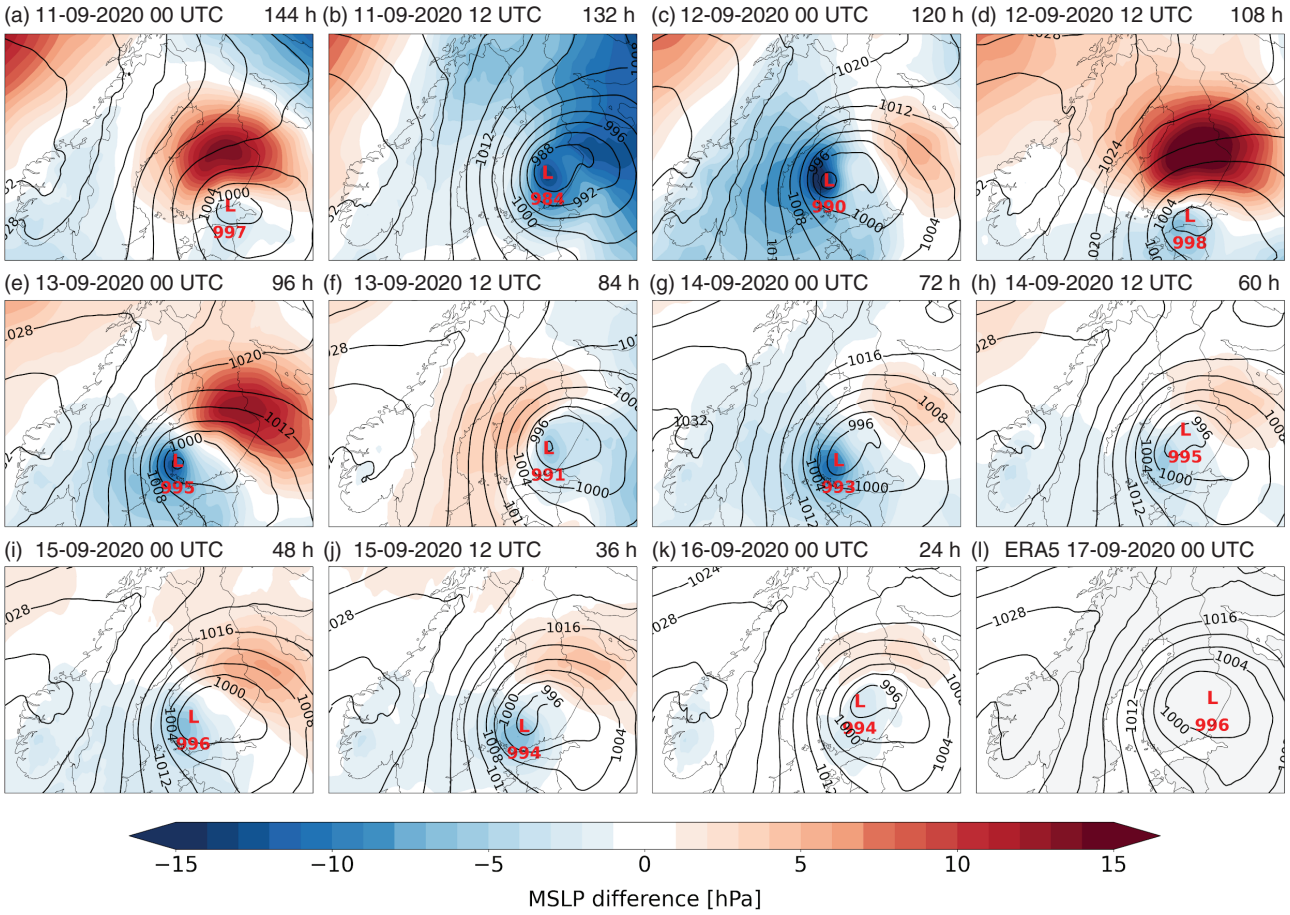

Figure 5. Mean sea level pressure (contours) from IFS forecasts and their difference from ERA5 reanalysis (colours) at different forecast lead times (a–k). The initialisation times and lead times of the forecasts are shown as titles of the panel figures. The valid time of all panels is 17 September 2020, 0000 UTC, which is shown in the last panel (l).

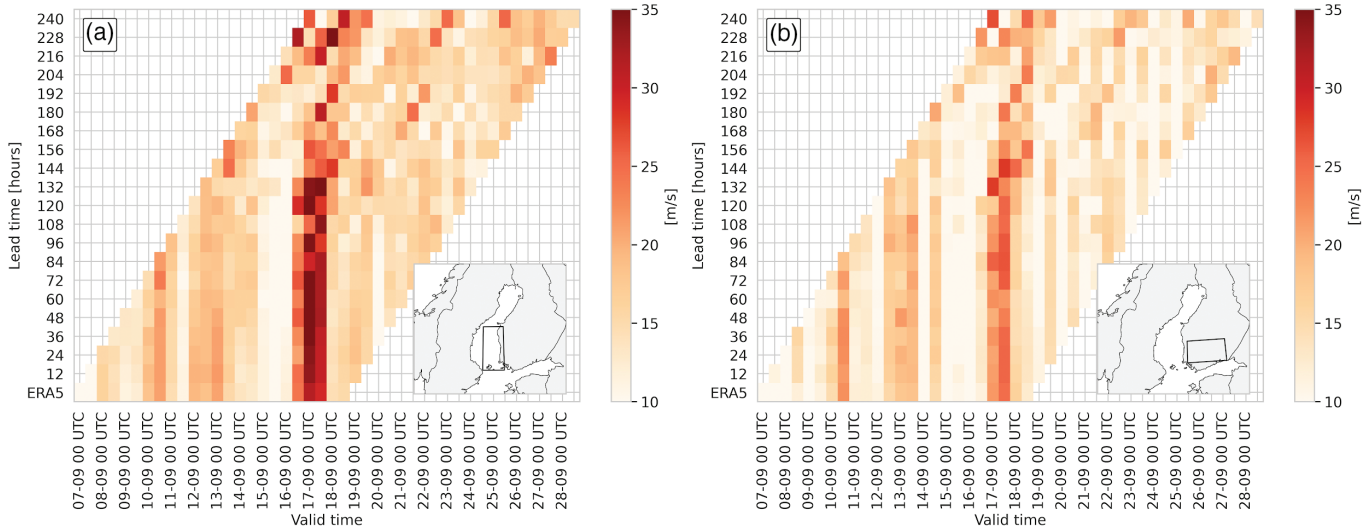

Figure 6. The spatial maximum of 10-metre wind gust speed as a function of valid time (x-axis) and forecast lead time (y-axis). Left panel (a) shows the maximum for the sea in western coast of Finland, and right panel (b) the maximum for the land in southern Finland. These areas are shown in the small plots. Note that 10-metre wind gusts are the maxima in the last 1 hour for 0–90 hours lead times, 3 hour for 90–144 hours lead times and 6 hour for 144–240 hours lead times. The values according to ERA5, which is considered here as a truth, are shown at the bottom row.

1200 UTC, the magnitude of the wind gusts were forecast quite well, with some modest underestimation at 48–60 hour lead times.

In order to assess how well ERA5 and IFS represent the real, observed wind speeds during storm *Aila*, Figure 7 shows the time series of maximum wind gust speed at two stations: Pietarsaari Kallan (Figure 7a) and Rauma Kylmäpihlaja (Figure 7b). The locations of these two stations are marked in Figure 2. They were selected because they recorded the highest wind speeds during storm *Aila*. Compared with ERA5, the IFS forecast initialised on 15 September 0000 UTC slightly underestimated the windiness in Pietarsaari (Figure 7(a)), while in Rauma the IFS forecast overestimated the peak gusts (Figure 7b). This is in line with Figure 5(i),

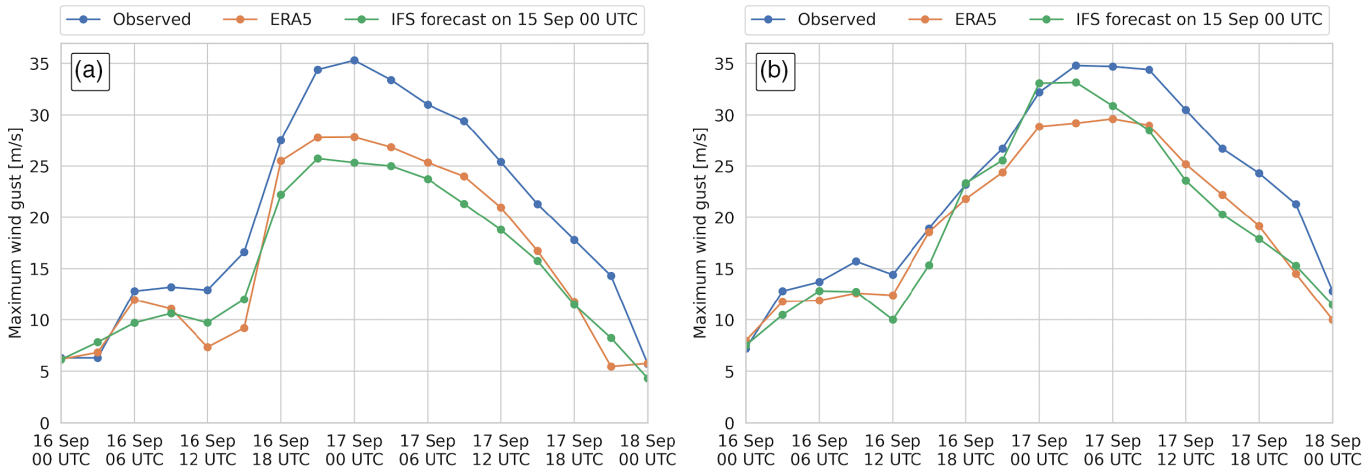

Figure 7. Maximum wind gust according to observations (blue), ERA5 reanalysis (orange) and IFS HRES forecast initialised on 15 September 0000 UTC (green) in (a) Pietarsaari Kallan and (b) Rauma Kylmäpihlaja. ERA5 and IFS forecasts are values from the nearest grid point to the weather station. The wind gusts in ERA5 and IFS represent the values at the altitude of 10m, while the observations in Pietarsaari Kallan (a) are done at 30m and Rauma Kylmäpihlaja (b) at 38m altitude.

which shows that the centre of the storm in the IFS forecast on 15 September 0000 UTC was predicted to be further west, indicating a stronger pressure gradient and thus stronger winds near Rauma on 17 September 0000 UTC. In reality, the centre of the storm on 17 September 0000 UTC was located in eastern Finland (Figure 5l) and hence most of the short-term forecasts, including the one initialised on 15 September 0000 UTC (Figure 7b), overestimated the windiness along the western coast (Figure 6a). Nevertheless, although having some errors in magnitude, the IFS forecast on 15 September 0000 UTC captured fairly well the temporal evolution of wind gusts at both stations.

The observed values are not fully comparable to ERA5 and IFS for two reasons. First, the observations are point values, while both ERA5 and IFS represent spatial averages from a 0.25° grid cell which is nearest to the weather stations. Secondly, the observations are made on isolated islands, on top of lighthouses, at 30 metres altitude (Pietarsaari Kallan, Figure 7(a)) and 38m altitude (Rauma Kylmäpihlaja, Figure 7(b)) while ERA5 and IFS represent 10-metres wind gust values. The ERA5 land-sea mask for Pietarsaari grid point is 0.43 and for Rauma grid point 0.23. This means that the model interprets the Pietarsaari grid point as almost half land while the observations represent pure marine conditions. For these reasons, the observed wind gusts are 3–7ms^{-1} higher than the modelled wind gusts, especially in Pietarsaari where the fraction of land in the model is higher (Figure 7(a)).

Wind speed comparison to climatology

During storm *Aila*, the highest wind speeds were observed along the western coast of Finland (Figure 2). Out of all stations, the maxima were recorded in Rauma

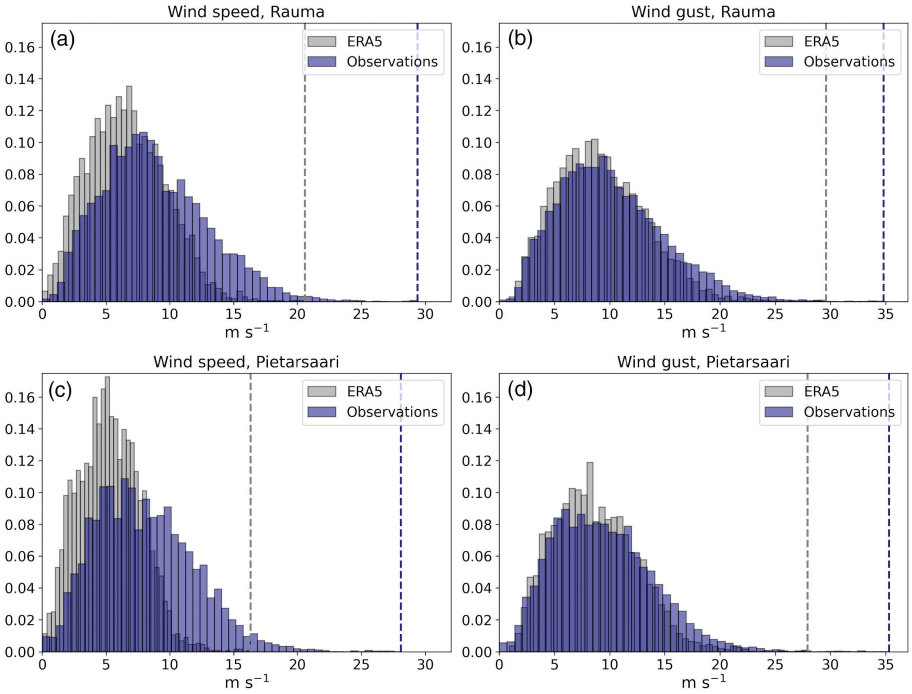

Figure 8. Wind speed (left panel) and wind gust (right panel) distributions in September during 2004–2020 based on ERA5 and observations in (a, b) Rauma Kylmäpihlaja and (c, d) Pietarsaari Kallan (the station locations are marked in Figure 2). The dashed vertical line denotes the maximum wind speed or wind gust in the chosen dataset.

Kylmäpihlaja with 29.4ms^{-1} (57kn) 10-minute average wind speed and 34.8ms^{-1} (68kn) wind gust (Figure 7(b)) and Pietarsaari Kallan with 28.1ms^{-1} (55kn) 10-minute average wind speed and 35.3ms^{-1} (69kn) wind gust (Figure 7(a)). We investigated the historical distributions of the wind speeds at these two stations in more detail in order to put the observed values into a climatological context. The comparison is made against September climatology, because *Aila* occurred in the middle of September.

Figure 8 shows histograms of the 1-hour maximum wind speed and wind gust for all observations from all Septembers 2004–2020 from both stations. In addition, the strongest ever observed wind speed and wind gust in all Septembers from 2004–2020 are shown as blue vertical lines in Figure 8. At both stations, the strongest observed winds and gusts during the entire 17-year period (2004–2020) occurred during storm *Aila*. Similarly, at the closest grid points to these stations in ERA5, the highest winds and gusts are associated with storm *Aila* (grey vertical lines in Figure 8). We also investigated a longer time period of 1979–2020 from ERA5 (not shown) and a similar result was found. Therefore, we can conclude that storm *Aila* had the strongest wind speeds

and wind gusts out of all Septembers in the observation record in 2004–2020 and in ERA5 in the period 1979–2020.

Furthermore, when the maximum wind speeds in all marine and land stations in Finland (excluding mountainous stations which are located over 200 m above sea level) during the whole observational history are considered, no higher September wind speeds are found (not shown). Thus, the observed wind speeds during *Aila* were records not only at Pietarsaari and Rauma stations (Figures 2, 7 and 8), but for the whole country. However, the caveat in this conclusion is that the observational network of wind speeds in Finland in the twentieth century was more sparse and only instantaneous values were recorded at certain times of the day. Thus, historic observations are likely biased towards lower wind speeds and the comparison must be interpreted with caution.

When comparing the wind distributions between the observations and ERA5 (Figure 8), the wind speeds are weaker and the distributions are less skewed to the right (i.e. narrower distribution) in ERA5 than in the observations. This may be due to the coarser resolution of ERA5, the difference in the wind speed level (10m in ERA5, 30–38m at the stations) and the local features which are not fully resolved in ERA5. Moreover, ERA5 captures the wind gust distribution better than the mean wind speed distribution. In the IFS, the wind gust parameter is calculated by summing up three terms: 10-metre wind speed, a term which represents surface roughness and boundary layer stability, and a convection term (ECMWF, 2013). Therefore, we suggest that while the 10-metre wind speeds are underestimated, some other term in the gust parametrisation, likely the roughness term, is overestimated, meaning that the two errors (of opposite sign) compensate each other. These are, however, values from only two stations and two grid points near the coast and may not represent a larger area over sea or land. This issue needs further research which is out of scope of this study. Furthermore, our finding that both mean and gust wind speeds in ERA5 are negatively biased in the right tail of the distributions (i.e. at high wind speeds) is in agreement with ERA5 wind distributions found in Sweden (Minola *et al.*, 2020).

Conclusions

Storm *Aila* was a severe autumn windstorm in Finland, affecting mainly the western and southern part of the country. According to preliminary estimations, *Aila* destroyed about half a million cubic metres of forestry, left 160 000 households without electricity and caused 2950 call outs for the emergency services.

The development of storm *Aila* was typical for baroclinic cyclones. The storm formed from a pre-existing frontal boundary under upper-level forcing and in a right entrance region of the jet stream. The formation of the surface low occurred only 18 hours before *Aila* hit Finland, which means that *Aila*'s deepening was still in progress as it arrived in Finland. Although storm *Aila* was exceptional in terms of its associated winds with substantial impacts, meteorologically *Aila* was not a deep storm and its deepening cannot be classified as an explosive.

The medium-range forecasts by ECMWF predicted the formation of storm *Aila* very well and meteorologists at FMI were able to issue warnings with moderately long lead times. For example, the first red warning (the highest level) was announced three days in advance, which indicates both high predictability and high impacts of the event. What is remarkable is that the storm itself formed only 30 hours before hitting Finland on 17 September 0000 UTC at its full strength, which means that the IFS model captured the potential development of the storm several days in advance. We speculate that the relatively large spatial scale of the developing storm and presumably the dominance of the adiabatic contributions (e.g., vorticity advection) over the diabatic processes were largely the reasons for the high level of predictability.

The observed wind speeds during storm *Aila* were exceptional for the time of the year. The maximum mean wind speed and gust wind speed were not only new September records for the weather stations where the readings were observed, but also for Finland as a whole for September. Although slightly higher wind speeds have been observed later in the year when windstorms are usually stronger, storm *Aila* belongs to the category of most notable windstorms in Finland. Luckily, *Aila* was well forecast, communicated and adequate preparations were made in time.

Acknowledgements

We thank Ville Siiskonen for retrieving the observational data for our use. ECMWF is acknowledged for making the IFS forecasts available and Copernicus is acknowledged for making ERA5 reanalysis available. This work was partly supported by the Ministry of the Environment (SUOMI-hanke), Ministry of the Agriculture and Forestry (MONITUHO), and The Atmosphere and Climate Competence Center (ACCC).

References

European Centre for Medium-Range Weather Forecasts (ECMWF). 2013. *IFS documentation CY38R1 Part IV: Physical processes*. Reading: ECMWF, pp. 51–52. Available at: https://www.ecmwf.int/node/9245 [accessed 5 November 2020].

Finnish Forest Centre (FFC). 2020. *Aila-myrsky kaatoi metsiä pääasiassa Pohjanlahden rannikkoalueelta*. Finnish Forest Centre press release. Available at: https://www.metsakeskus.fi/uutiset/aila-myrsky-kaatoi-metsia-paaasiassa-pohjanlahden-rannikkoalueelta [accessed 5 November 2020].

Finnish Meteorological Institute (FMI). 2020. *Aila-myrsky oli vaikutuksiltaan hyvin merkittävä*. FMI press release. Available at: https://www.ilmatieteenlaitos.fi/tiedote/3Zz47oU1YX2YQwZhw5ws9n [accessed 2 November 2020].

Gregow H, **Rantanen M**, **Laurila TK**, **Mäkelä A**. 2020. *Review on winds, extratropical cyclones and their impacts in Northern Europe and Finland*. Finnish Meteorological Institute Reports, 2020(3). Available at: http://hdl.handle.net/10138/320298. [accessed 5 November 2020].

Hersbach H, **Bell B**, **Berrisford P**, **Hirahara S**, **Horányi A**, **Muñoz-Sabater J**. ***et al***. 2020. The ERA5 global reanalysis. *Quarterly Journal of the Royal Meteorological Society*, **146:** 1999–2049.

Kufeoglu S. **Lehtonen M**. 2014. Cyclone Dagmar of 2011 and its impacts in Finland. In *IEEE PESInnovative Smart Grid Technologies, Europe*, pp. 1–6. https://doi.org/10.1109/ISGTEurope.2014.7028868.

Lackmann G. 2011. *Midlatitude synoptic meteorology - Dynamics, analysis and forecasting*. American Meteorological Society: MA, USA.

Láng I, **Mäkelä A**, **Korpela P**, **Gregow H**. (submitted) Windstorm Aila 2020: Societal impacts. *FMI's Climate Bulletin: Research Letters*.

Laurila TK, **Sinclair VA**, **Gregow H**. 2020. The extratropical transition of Hurricane Debby (1982) and the subsequent development of an intense windstorm over Finland. *Mon. Wea. Revi.* **148:** 377–401.

Minola L, **Zhang F**, **Azorin-Molina C**, **Safaei PA**, **Flay RGJ**, **Hersbach H**. ***et al***. 2020. Near-surface mean and gust wind speeds in ERA5 across Sweden: Towards an improved gust parametrization. *Climate Dynamics*, **55:** 887–907.

Sainsbury EM, **Schiemann RK**, **Hodges KI**, **Shaffrey LC**, **Baker AJ**, **Bhatia KT**. 2020. How important are post-tropical cyclones for European windstorm risk? *Geophys. Res. Lett.* **47:** e2020GL089853.

Tollman N, **Lehtonen I**, **Gregow H**. 2019. Aapeli-myrsky rikkoi ennätyksiä. *FMI's Clim. Bull.* **2019:** 8–9.

Valta H, **Lehtonen I**, **Laurila TK**, **Venäläinen A**, **Laapas M**, **Gregow H**. 2019. Communicating the amount of windstorm induced forest damage by the maximum wind gust speed in Finland. *Adv. Sci. Res.* **16:** 31–37.

Correspondence to: Mika Rantanen

mika.rantanen@fmi.fi

© 2021 The Author. Weather published by John Wiley & Sons Ltd on behalf of the Royal Meteorological Society

This is an open access article under the terms of the Creative Commons Attribution License, which permits use, distribution and reproduction in any medium, provided the original work is properly cited.

doi: 10.1002/wea.3943